Prediction of Mouse Senescence from HE-Stain Liver Images Using an Ensemble SVM Classifier

Hui-Ling Huang[1,2], Ming-Hsin Hsu[2], Hua-Chin Lee[1], Phasit Charoenkwan[2], Shinn-Jang Ho[3], and Shinn-Ying Ho[1,2,*]

[1] Department of Biological Science and Technology,
National Chiao Tung University, Hsinchu, Taiwan
[2] Institute of Bioinformatics and Systems Biology,
National Chiao Tung University, Hsinchu, Taiwan
[3] Department of Automation Engineering,
National Huwei Institute of Technology, Yunlin, Taiwan
hlhuang@mail.nctu.edu.tw, morris679@yahoo.com.tw,
huachinlee@g2.nctu.edu.tw, phaznexus@hotmail.com,
sjho@nfu.edu.tw, syho@mail.nctu.edu.tw

Abstract. Study of cellular senescence from images in molecular level plays an important role in understanding the molecular basis of ageing. It is desirable to know the morphological variation between young and senescent cells. This study proposes an ensemble support vector machine (SVM) based classifier with a novel set of image features to predict mouse senescence from HE-stain liver images categorized into four classes. For the across-subject prediction that all images of the same mouse are divided into training and test images, the test accuracy is as high as 97.01% by selecting an optimal set of informative image features using an intelligent genetic algorithm. For the leave-one-subject-out prediction that the test mouse is not involved in the training images of 20 mice, we identified eight informative feature sets and established eight SVM classifiers with a single feature set. The best accuracy of using an SVM classifier is 71.73% and the ensemble classifier consisting of these eight SVM classifiers can advance performance with accuracy of 80.95%. The best two feature sets are the gray level correlation matrix for describing texture and Haralick texture set, which are good morphological features in studying cellular senescence.

Keywords: Aging, cellular senescence, feature selection, genetic algorithm, HE-stain, image analysis, prediction, SVM.

1 Introduction

Research of cellular senescence has been studied for more than 40 years. There are many literatures which point the differences between young and senescent cells in molecular level. In morphological way, the changes on surface of senescent cells are observed. With quantification of variation, seldom studies were proposed to solve the problem of identifying senescence from images in molecular level. Predicting the hierarchy of senescence by HE-stain images plays an important role in studying cellular senescence.

A. Selamat et al. (Eds.): ACIIDS 2013, Part II, LNAI 7803, pp. 325–334, 2013.

An increasing proportion of the healthcare budget is devoted to the growing geriatric population, so it is essential to understand the molecular basis of ageing and identify possible avenues for therapeutic intervention [1]. Cellular senescence has been studied since the research [2] which showed that the senescent cells enlarged more than twofold relative to non-senescent counterpart. In addition to losing the ability to divide, cells in the senescent state exhibit dramatic alterations in morphology, mass, and dynamics of their subcellular organelles, and thereby display structural and functional differences compared to proliferating cells. These differences include an enlarged and flat cellular morphology, increased reactive oxygen species (ROS) production [3], and the accumulation of resultant ROS-mediated damage products such as: (1) lipofuscins and granular particles [4], (2) altered mass and functionality of mitochondria and lysosomes [5], and (3) certain cytosolic and nuclear markers such as senescence associated-b-galactosidase activity (SA-b-Gal) and senescence-associated heterochromatin foci (SAHF) [6].

For predicting mouse senescence and further analyzing the molecular basis of ageing, we used HE-stain liver images categorized into four classes (1 month, 6 months, 16 months, and 24 months) obtained from a public dataset. To design an accurate classifier for senescence prediction, there are three essential tasks: 1) identification of an informative image feature set, 2) determination of selecting an efficient classifier, and 3) development of an effective strategy for coping with the leave-one-subject-out prediction considering the variation of mouse aging.

Considering the aforementioned three tasks, we propose an optimized image feature selection method using an intelligent genetic algorithm for automatically identifying an informative image feature set. At first, we established a number of feature sets which maybe relate to morphology of senescent cells. The feature selection and classifier design are done at the same time. By comparing the widely-used support vector machine (SVM) with the selected feature set, SVM is adopted in the consequent study. Finally, this study proposes an SVM-based classifier with a novel set of grey-level image features to predict mouse senescence from HE-stain liver images.

2 Related Work

In these alterations showed in senescent cells, some could be displayed by hematoxylin and eosin staining, i.e. lipofuscin [7]. The accumulations of highly cross-linked protein are thought to relate to chronic oxidative stress and a failure to degrade damaged and denatured proteins [8]. Besides the highly oxidized insoluble proteins, senescence-induced nuclear defects resulted from accumulation of lamin A/C show the differences between young and old individuals [9]. In morphological perception, the large cell change frequently found in liver biopsy specimens from old subjects would represent senescent hepatocytes with HE stain [10].

Pasquinelli et al verified the possible influence of age in healthy liver parenchyma on DwI-related parameters: apparent diffusion coefficient, perfusion fraction, diffusion and pseudodiffusion coefficient [11]. Fonseca et al identified structural remodeling in human saphenous veins by applying histochemistry, fluorescence staining and

quantitative image analysis to specifically assess intimal area, intimal cellularity and intimal collagen content and organization [12]. In the study of Udono et al, they mentioned that high content screening (HCS)-based image analysis is becoming an important and powerful research tool. An automated and quantitative cellular image-analysis system was employed in their study to quantify the cellular senescence phenotypes induced in normal human diploid fibroblasts, TIG-1 cells, and found to be a powerful tool in the cellular senescence study [13].

On the other hand, there are some literatures that proposed a computational method for both quantitatively predicting and analyzing. Driscoll et al show a novel, automated and high throughput nuclear shape analysis that quantitatively measures curvature, area, perimeter, eccentricity and additional metrics of nuclear morphology for large populations of cells [14]. Choi et al used automated segmentation and shape analyses, with pre-defined features and with computer generated components, to compare nuclei from various premature aging disorders caused by alterations in nuclear proteins [15]. Shamir et al proposed to use the image texture entropy as an objective measurement that reflects the structural deterioration of the C. elegans muscle tissues during aging [16]. Johnston et al considered changes in overall morphology to quantitatively track tissue architecture during adulthood and aging in the C. elegans pharynx, the neuromuscular feeding organ [17]. All of the related works are listed in Table 1.

Table 1. Related work of studying cellular senescence

References	Aging related	Main type of method	Prediction	Objects of study
[11]	Yes	Biological	No	Human saphenous vein
[12]	Yes	Biological	No	Human diploid fibroblast
[13]	Yes	Biological and mathematical	No	Human liver parenchymas
[14]	Yes	Biological	No	Human diploid fibroblast and mouse tail fibroblast
[15]	Yes	Biological and computational	No	Human dermal fibroblast
[16]	Yes	Computational	No	Nuclei of human cells and mouse model
[17]	Yes	Computational	No	Pharynx of C. elegans
Ours	Yes	Computational	Yes	Mouse liver biopsy specimen images of HE stain

3 Design Procedure

The original HE-stain images were preprocessed such as noise remove and grey level transformation. From Fig. 1, the core technique IBCGA and SVM with feature selection were used for determining the optimized feature set with best accuracy. The feature extraction tool is developed for extracting the features from the bio-medical or tissue images by using the inheritable bi-objective combinatorial genetic algorithm (IBCGA) [18][19] as the core technique. The feature extraction tool designed by authors is a general purpose tool in the image informatics field and can automatically extract the image features categorized into three parts: shape features, texture features and wavelet features. The shape features include boundary moment, Zernike moment,

Morphological, Regional property and Tchebichef moment. The texture features include Haralick, Gray level co-occurrence matrix (GLCM), Gabor filter, Tamura, Granularity, Intensity and Fourier; wavelet feature includes Haar and Daubichies. In addition, each feature set has its own parameter setting to be defined depending on usages and applications, such as degree, radius, histogram bin, max distance or distance gap. For different predicting aims, across subject and leave one subject out are designed to prediction and analysis HE-stain images.

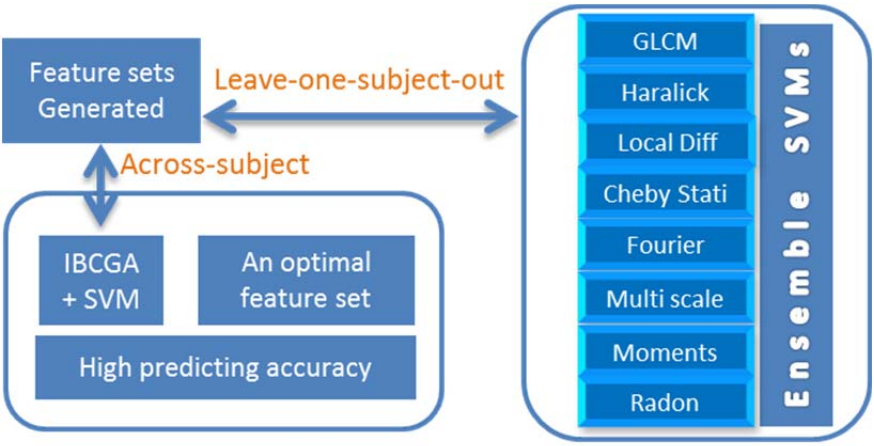

Fig. 1. Design procedures of the system. The proposed feature sets are used to design and evaluate the proposed method.

3.1 Selecting an Informative Feature Set

The core of IBCGA optimizes classification accuracy and minimizes number of features [18]. The intelligent genetic algorithm uses a divide-and-conquer strategy and an orthogonal array crossover to efficiently solve large-scale parameter optimization problems. IBCGA can efficiently explore and exploit the search space of $C(n, r) = n!/[(n-r)!r!]$. IBCGA can efficiently search the space of $C(n, r \pm 1)$ by inheriting a good solution in the space of $C(n, r)$ [18]. The proposed chromosome encoding scheme of IBCGA consists of both binary genes for feature selection and parametric genes for tuning SVM parameters.

The fitness function is the guide for IBCGA to acquire solutions with best performance. The fitness function of IBCGA is the 5-CV overall accuracy. IBCGA with the fitness function $f(X)$ can simultaneously obtain a set of solutions, X_r, where $r=r_{start}$, $r_{start}+1$, …, r_{end} in a single run. The algorithm of IBCGA with the given values r_{start} and r_{end} is described as follows:

Step 1) (Initiation) Randomly generate the initial population of N_{pop} individuals. All the n binary genes have r 1's and n-r 0's where $r = r_{start}$.

Step 2) (Evaluation) Evaluate the values of fitness for all individuals using $f(X)$.

Step 3) (Selection) Use the traditional tournament selection which chooses the winner from two randomly selected individuals to form a mating pool.

Step 4) (Crossover) Select $p_c \cdot N_{pop}$ parents from the mating pool and perform orthogonal array crossover on the selected pairs of parents where p_c is the crossover probability.

Step 5) (Mutation) Apply the swap mutation operator to the randomly selected $p_m \cdot N_{pop}$ individuals in the new population where p_m is the mutation probability. To prevent the best fitness value from deteriorating, mutation is not applied to the best individual.

Step 6) (Termination test) If the stopping condition for obtaining the solution X_r is satisfied, output the best individual as X_r. Otherwise, go to Step 2). In this study, the stopping condition is to perform 60 generations.

Step 7) (Inheritance) If $r < r_{end}$, randomly change one bit in the binary genes for each individual from 0 to 1; increase the number r by one, and go to Step 2). Otherwise, stop the algorithm.

3.2 Ensemble SVM Classifiers

In this study, the number of mice is relatively small, compared with the complex of recognition problems in the HE-stain liver images. For coping with the unknown subject problem, the ensemble SVM classifier consisting of k SVM classifiers and a voting method is developed to advance the prediction accuracy.

(1) SVM classifiers: The prediction accuracy is highly related to the selected feature set for every SVM classifier. The used types of features include: 1) GLCM, 2) Haralick, 3) Local Diff, 4) Cheby Statis, 5), Fourier 6) Multi scale, 7) Moments, and 8) Radon. Each SVM classifier uses one type of features.

(2) Voting method: Different classification results of the query sequences will be obtained from the outputs of the k independent SVM classifiers, and then these results are integrated using the simple voting method.

$$\mathrm{FS}_j = \sum_{i=1}^{k} \tau, \quad \tau = \begin{cases} 1, & C_i = j \\ 0, & otherwise \end{cases}, \tag{1}$$

where k (=8 in this study) is the number of SVM classifiers, j=1, 2, …, C (C=4 in this study) is the class label, C_i is the predicted class label by the ith SVM classifier. The final class is determined by argmax $\{\mathrm{FS}_1, \mathrm{FS}_2, \mathrm{FS}_3, \mathrm{FS}_4\}$.

4 Dataset

The mouse liver biopsy specimen images are provided by IICBU 2008 [19]. Fifty color images per liver were manually acquired using a Carl Zeiss Axiovert 200

microscope and 40x objective. Therefore, 1500 images from 30 livers were collected, and each image was converted into a gray-scale TIFF image. We use both male- and female-mouse of 1 month, 6 months, 16 months and 24 months in ad-libitum diet (Table 2), and all the images were HE-stain images. A single mouse has prepared all imaging and staining for leading to a small variability. Finally, there are 1027 images from 21 mice to be used for analysis.

In this study, two prediction methods are investigated for understanding the informative image features and the relationship between cell morphology and cellular senescence. For the across-subject prediction that all images of the same mouse are randomly divided into training (5/6) and test images (1/6). For the leave-one-subject-out prediction that the test mouse is not involved in the training images of 20 mice. The prediction accuracy is the mean of 21 predictions where each mouse is served as a test mouse.

Table 2. The number of individuals in each classes and number of images for each individauls

	Class no.										
	1		2			3			4		
Individual	4		6			5			6		
Images	50	50	50	50	15	50	61	51	50	51	50
	50	50	50	50	50	50	50		49	50	50

5 Results

5.1 Across-Subject Prediction

Table 3 shows the results of 30 independent runs. The averaged training and test accuracies are 98.80% and 97.01%, respectively. With the same dataset, the results of using the existing Wnd-charm feature set are shown in Table 4. The results show that the averaged training and test accuracies are 93% and 88%, respectively. The result reveals that the proposed method is better than the Wnd-charm method due to the feature selection of IBCGA. In the Wnd-charm method, the 601 features were chosen from default 4008 characteristics by using the Fisher score. However, IBCGA chooses 89.5 features on average as a feature set. From the features selected in the 30 runs (Table 4), there are four features which appear more than 15 times. The top 4 frequently-selected features are listed in Table 5.

Table 3. Results of 30 independent runs with the number of features selected by IBCGA

Run number	Training accuracy	Test accuracy	No. of elected features
1	99.07%	97.56%	42
2	98.84%	96.34%	94
3	98.38%	96.95%	133
4	99.19%	95.12%	75
5	98.03%	96.95%	111
6	98.73%	96.95%	57
7	98.61%	96.95%	74
8	98.61%	96.34%	38
9	98.96%	96.95%	139
10	98.84%	98.78%	100
11	98.73%	97.56%	78
12	98.73%	97.56%	88
13	98.49%	98.78%	123
14	98.84%	97.56%	104
15	98.03%	96.34%	69
16	98.73%	97.56%	148
17	98.73%	97.56%	111
18	99.07%	98.17%	39
19	99.07%	98.17%	49
20	98.38%	96.34%	98
21	99.30%	98.17%	33
22	98.73%	95.73%	149
23	99.19%	95.12%	40
24	99.07%	95.73%	52
25	99.54%	97.56%	141
26	98.84%	96.34%	133
27	98.61%	95.12%	114
28	99.19%	97.56%	47
29	98.84%	95.73%	79
30	98.73%	98.78%	126
Average	98.80%	97.01%	89.5

Table 4. The training and test results by using the Wnd-charm method

	Training	Independent test
Accuracy	93%	88%

Table 5. The top 4 feature sets with the highest selection frequency

Feature name (feature ID)	No. of appearances in the feature selection
Gabor_Standard deviation 3 (982)	16
Debeucies4_'W_h6' (1025)	16
Granularity_Standard deviation pixel distance 1 (1071)	19
Granularity_Standard deviation pixel distance 3 (1073)	17

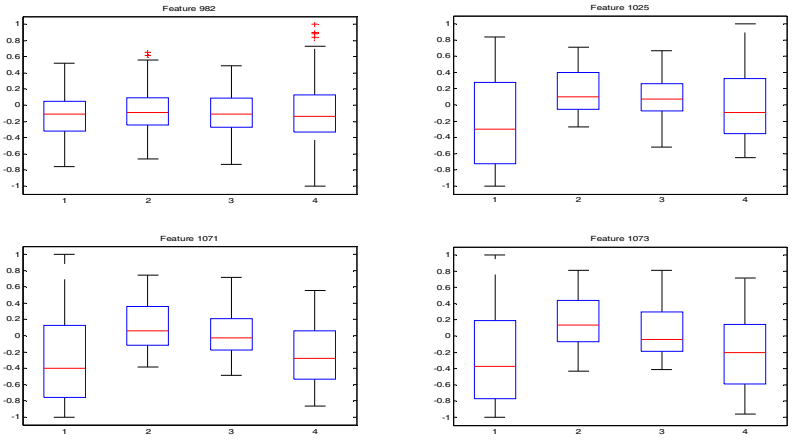

Fig. 2. Box plots of the four top-ranked features

Fig. 2 shows the box plot statistics of the top 4 features, and two of the top 4 features (features 1071 and 1073) are the texture characteristics from the dataset.

5.2 Feature Selection

IBCGA can automatically choose feature sets with preferred sizes from all candidate features. Fig. 3 shows the feature selection results with accuracy. Finally, we choose 10 features as one feature set with accuracy of 93.29%.

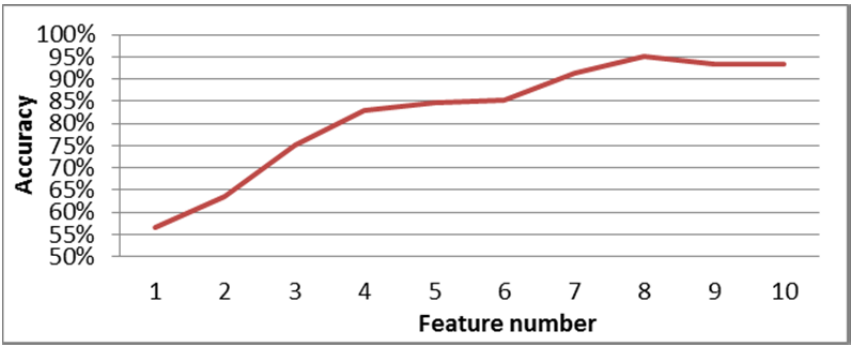

Fig. 3. Feature selection from 1 to 10 features using IBCGA

5.3 Ensemble Classifier

For the leave-one-subject-out prediction that the test mouse is not involved in the training images of 20 mice, we identified eight informative feature sets and established eight SVM classifiers with a single feature set, shown in Table 6. The best accuracy of using an SVM classifier is 61.90% and the ensemble classifier consisting of these eight SVM classifiers can advance performance with accuracy of 80.95%.

The best two feature sets are the gray level correlation matrix for describing texture and Haralick texture set, which are good morphological features in studying cellular senescence.

Table 6. Leave-one-subject-out prediction results

Feature	GLCM	Haralick	Local Diff.	Cheby Statis
ACC	61.90%	57.14%	19.05%	47.62%

Feature	Cheby Fourier	Multi scale	First 4 moments	Radon	Ensemble
ACC	19.05%	38.10%	28.57%	33.33%	80.95%

The two best features are discussed as follows:

1. Gray level correlation matrices (GLCM)
GLCM set was used for describing texture of tissue [21]. It could express the relation between pixels. The probability value in GLCM will directly use as texture features. The level for histogram with 32 bins is usually the multiple times of 8. So here we set level to 8 and maximum distance to 5, which allows the total feature number to 1280.

2. Haralick texture set
Haralick texture set was published by Haralick, R.M. at 1973 [21]. Haralick defines fourteen statistical measurements calculated from GLCM. In this study, additional four statistical formulae are also used. Because it is based on GLCM, so the parameter settings are the same with those of GLCM.

6 Conclusions

We have proposed an ensemble support vector machine (SVM) based classifier with a novel set of image features to predict mouse senescence from HE-stain liver images categorized into four classes. The informative image features are obtained using the optimized feature selection algorithm IBCGA. The GLCM and GLCM-based Haralick texture set are good morphological features in studying cellular senescence. The ensemble SVM classifier performs well, compared with existing methods. For the leave-one-subject-out prediction, the ensemble approach can efficiently advance accuracy, compared with the non-ensemble approach. This study investigates classifiers and various sets of features on grey-level images. The future work is to investigate color-based feature sets for further analyzing the senescent cells.

References

1. Martin, J.E., Sheaff, M.T.: The pathology of ageing: concepts and mechanisms. J. Pathol 211(2), 111–113 (2007)
2. Hayflick, L.: The Limited in Vitro Lifetime of Human Diploid Cell Strains. Exp. Cell Res. 37, 614–636 (1965)
3. Kurz, T., et al.: Lysosomes and oxidative stress in aging and apoptosis. Biochim. Biophys. Acta 1780(11), 1291–1303 (2008)

4. Schmucker, D.L., Sachs, H.: Quantifying dense bodies and lipofuscin during aging: a morphologist's perspective. Arch Gerontol Geriatr 34(3), 249–261 (2002)
5. Terman, A., et al.: Mitochondrial recycling and aging of cardiac myocytes: the role of autophagocytosis. Exp. Gerontol. 38(8), 863–876 (2003)
6. Braig, M., et al.: Oncogene-induced senescence as an initial barrier in lymphoma development. Nature 436(7051), 660–665 (2005)
7. Hoare, M., Das, T., Alexander, G.: Ageing, telomeres, senescence, and liver injury. J. Hepatol. 53(5), 950–961 (2010)
8. Jung, T., Bader, N., Grune, T.: Lipofuscin: formation, distribution, and metabolic consequences. Ann. N. Y. Acad. Sci. 1119, 97–111 (2007)
9. Scaffidi, P., Misteli, T.: Lamin A-dependent nuclear defects in human aging. Science 312(5776), 1059–1063 (2006)
10. Ikeda, H., et al.: Large cell change of hepatocytes in chronic viral hepatitis represents a senescent-related lesion. Human Pathology 40(12), 1774–1782 (2009)
11. Pasquinelli, F., et al.: Magnetic resonance diffusion-weighted imaging: quantitative evaluation of age-related changes in healthy liver parenchyma. Magnetic Resonance Imaging 29(6), 805–812 (2011)
12. Fonseca, C., et al.: The effects of aging on the intimal region of the human saphenous vein: insights from multimodal microscopy and quantitative image analysis. Histochem. Cell Biol. (2012)
13. Udono, M., et al.: Quantitative analysis of cellular senescence phenotypes using an imaging cytometer. Methods 56(3), 383–388 (2012)
14. Driscoll, M.K., et al.: Automated image analysis of nuclear shape: what can we learn from a prematurely aged cell? Aging (Albany NY) 4(2), 119–132 (2012)
15. Choi, S., et al.: Computational image analysis of nuclear morphology associated with various nuclear-specific aging disorders. Nucleus 2(6), 570–579 (2011)
16. Shamir, L., Wolkow, C.A., Goldberg, I.G.: Quantitative measurement of aging using image texture entropy. Bioinformatics 25(23), 3060–3063 (2009)
17. Johnston, J., et al.: Quantitative Image Analysis Reveals Distinct Structural Transitions during Aging in Caenorhabditis elegans Tissues. PLoS One 3(7) (2008)
18. Ho, S.-Y., Chen, J.-H., Huang, M.-H.: Inheritable genetic algorithm for biobjective 0/1 combinatorial optimization problems and its applications. IEEE Trans. Syst. Man Cybern. B Cybern. 34(1), 609–620 (2004)
19. Ho, S.-Y., Shu, L.-S., Chen, J.-H.: Intelligent evolutionary algorithms for large parameter optimization problems. IEEE Trans. on Evol. Comp. 8(6), 522–541 (2004)
20. Shamir, L., et al.: IICBU 2008: a proposed benchmark suite for biological image analysis. Med. Biol. Eng. Comput. 46(9), 943–947 (2008)
21. Haralick, R.M., Shanmugam, K., Dinstein, I.: Textural features for image classification. IEEE Trans. on Systems, Man, and Cybernetics 6, 269–285 (1973)